JAAS

ROYAL SOCIETY OF CHEMISTRY

PAPER

View Article Online
View Journal | View Issue

Cite this: *J. Anal. At. Spectrom.*, 2024, **39**, 2767

Mg separation from samples with very high Ca/Mg ratios for Mg isotope analysis

Niklas Keller * and Michael Tatzel

Samples with very high Ca/Mg ratios present challenges for measuring their Mg isotope ratios. Here, we present an efficient method to separate Mg from samples with high Ca/Mg matrices, which also allows for quantitative separation of Sr, Ca and K. The method comprises a three-step chromatographic separation using DGA and AG50W-X12 (200–400 mesh) cation exchange resin. By utilising the automated sample purification system prepFAST MC™ for two of the three separations, the labour is substantially minimised. This analytical approach results in a quantitative Mg yield and a pure Mg solution, with other cations reduced to below the limit of detection (<53 ng mL^{-1}). We demonstrate the efficacy of this method using a set of geochemical reference materials with Ca/Mg ratios ranging from 1.32 to 1271 mol mol^{-1}. This approach enhances sample throughput and ensures high-quality separations in carbonate samples characterised by high Ca/Mg ratios.

Received 23rd July 2024
Accepted 2nd October 2024

DOI: 10.1039/d4ja00266k

rsc.li/jaas

Introduction

Magnesium (Mg) is a major element in the Earth's crust and the second most abundant cation in the ocean, and participates in key geochemical cycles at the Earth's surface. To trace processes such as rock weathering and diagenesis, Mg isotopes are a widely used tool and the main archives for them are carbonates. In speleothems they are used for studies of climate change in terrestrial settings,[1,2] in dolostones or dolomite-rich carbonates they serve as tracers for rock weathering, seawater chemistry and diagenesis.[1,3–11] Mg isotope variations in biogenic carbonates can also be used as proxies to study palaeoceanographic changes.[3,12–21]

Mg is closely linked to the carbon cycle due to processes like weathering of minerals and precipitation of carbonates and clays in the ocean, which are major controlling factors of both elements at the Earth's surface.[22] Because of this connection, Mg isotope analysis has gained particular interest and may provide valuable insights into the climatic past. Biogenic carbonates can record seawater Mg isotope ratios and thus serve as valuable archives for δ^{26}Mg (the normalized ^{26}Mg/^{24}Mg isotope ratio) of paleo-seawater and reveal the causes of the secular shift in Ca/Mg during the Cenozoic.[15,20,21]

The low Mg concentrations in most carbonate minerals challenge precise and accurate Mg isotope ratio analysis. Residual matrices and incomplete recovery of Mg can introduce significant bias into the measurements.[5] In dolomite (approx. 13 mol%) and in high-Mg calcite (>4 mol%) Mg is a major constituent[23] and poses no analytical challenge. These analyses are routinely conducted with a single-step chromatographic separation using mostly the AG50W-X12 resin. However, in low-Mg calcite Mg occurs as minor element (<4 mol%) and in aragonite only in trace amounts (<0.5 mol%) creating the necessity for a different separation routine. Various chromatographic separation techniques have been developed over the years using different cation exchange resins. The most commonly used cation exchange resin for Mg is AG50W-X12 from Bio-Rad. It is employed either in a single-step separation[1,24,25] or multiple-step separations.[3,26] Some studies have used AG50W-X8 (ref. 5 and 27) or AG MP-50.[18] Others have employed AG50W-X12 in multiple-step separations in combination with other resins, such as AG50W-X8,[4,28] AG MP-1M[29] or DGA (Triskem).[30]

These methods are only partially suitable for samples with a very high Ca/Mg ratio as they are prone to a non-quantitative collection of Mg if Ca is to generously collected. Recently, the DGA resin has been used in the purification of Mg and Ca[25,30] because it binds Ca and Sr, but not Mg. It also does not bind other elements such as K and Na as shown in the detailed overview of partition coefficients provide by Pourmand and Dauphas (2010) (ref. 31). We report a development of the method from Bao *et al.*, 2020 (ref. 30), which minimises labour by using the ESI prepFAST MC™ automatic sample purification system. Their method consists of two manually conducted chromatographic separations using DGA and AG50W-X12 and was tested only for samples with a lower Ca/Mg ratio than that of carbonates. We use the prepFAST MC™ system from ESI for the separation with the DGA resin. Benefits of this system are the minimisation of labour, an improvement of reproducibility, and an enhanced sample throughput.

Geowissenschaftliches Zentrum, Universität Göttingen, Goldschmidtstr. 1-3, 37077 Göttingen, Germany. E-mail: niklas.keller@uni-goettingen.de

Material and method

Material

We processed several carbonate reference materials with predominantly high Ca/Mg ratios ranging from 1.32 to 1271 mol mol^{-1}. For some reference materials, the Mg isotope ratios are known; for the others, they are reported here for the first time. The reference materials used include the limestones JLs-1 (Geological Survey of Japan, GSJ), IAEA-B7 (International Atomic Energy Agency, IAEA), and Cal-S (Centre de Recherches Petrographiques et Geochemique, France, CRPG); the dolomite JDo-1 (GSJ); two giant clams *Tridacna gigas* JCt-1 (GSJ) and EN-1 (United States Geological Survey, USGS); the coral *Porites* sp. JCp-1 (GSJ); the carbonatite standard COQ-1 (USGS); and the pure calcium carbonate standard BAM-RS3 (Bundesanstalt für Materialforschung und -prüfung (BAM), Germany). Table 1 lists the processed reference materials with their published Ca/Mg ratios and δ^{25}Mg and δ^{26}Mg values.

Sample preparation

Depending on their magnesium concentration, a total of 0.23–27.38 mg of solid sample was processed, corresponding to 3.12–26 μg Mg. The samples were dissolved in 1.5 mL HNO_3 (2 mol L^{-1}) and centrifuged to check for possible solid. In no case residues were observed. An aliquot of 0.5 mL was used for concentration measurement by ICP-OES. The only standard that was digested differently is the carbonatite COQ-1 because it did not dissolve completely in HNO_3. It was additionally treated with double-distilled HNO_3 (14 mol L^{-1}) + HF (23 mol L^{-1}) and heated up to 120 °C for 15 hours. Afterwards it was treated with double-distilled HCl (11 mol L^{-1}) until it dissolved completely. For the standard JCp-1, three replicates were processed and for BAM-RS3, four replicates were processed.

Chromatographic separation

The separation of elements is conducted with a three-step cation-exchange chromatography. The first two separations serve for the removal of the vast majority of Ca. This is done by using the DGA resin (50–100 μm) in the automated chromatographic system prepFAST MC™, which performs the chromatographic separation automatically and runs each sample over a single column consecutively. Acids, volumes, and flow rates can be adjusted for each method, allowing for precise separation. The samples are loaded in 1 mL HNO_3 (2 mol L^{-1})

Table 1 All processed reference materials with their respective literature Ca/Mg ratios and their Mg isotope ratios. BAM-RS3 and IAEA-B7 have no published δ^{25}Mg and δ^{26}Mg values

Standard	Material	Ca/Mg (mol mol^{-1})	δ^{25}Mg (‰ DSM3)	2*s*	δ^{26}Mg (‰ DSM3)	2*s*	Reference
BAM-RS3	Calcium carbonate	1271					35
JCt-1	*Tridacna gigas*	740	−1.72	0.01	−3.37	0.01	35
EN-1	*Tridacna gigas*	740[a]	−2.23	0.02	−4.39	0.02	32
JCp-1	*Porites* sp.	239	−1.03	0.02	−1.96	0.04	35
IAEA-B7	Limestone	131					33
Cal-S	Limestone	109	−2.25	0.11	−4.37	0.14	35
JLs-1	Limestone	65	−1.86	0.05	−3.60	0.07	32 and 35
COQ-1	Carbonatite	28	−0.25	0.04	−0.50	0.06	27 and 34
JDo-1	Dolomite	1.32	−1.23	0.09	−2.35	0.15	35

[a] Same ratio as JCt-1 assumed. If available, values were obtained from GeoReM.

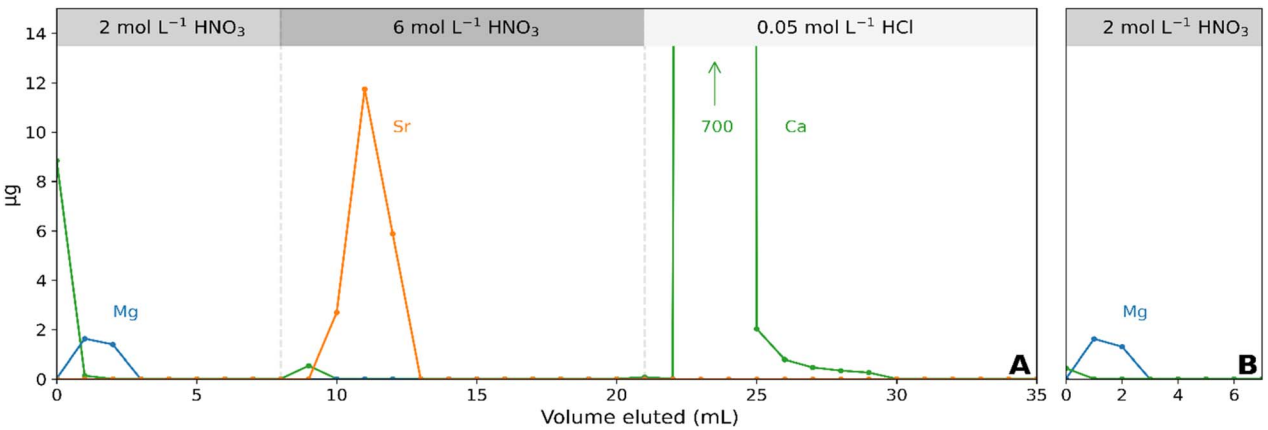

Fig. 1 Elution profiles of aragonite (JCp-1) processed over the DGA resin using the automated prepFAST MC™ system (conditions summarised in Table 2). (A): The first chromatographic step separates Mg, Sr and Ca, where the Ca/Mg ratio is reduced from 240 mol mol^{-1} to about 5 mol mol^{-1}. The usage of a high fraction of the exchange capacity (approx. 40%), leads to Ca breakthrough and elution with the Mg fraction. (B): The repeated procedure further decreases the Ca/Mg ratio to approx. 0.26 mol mol^{-1}. Sr is quantitatively separated in the first pass.

Table 2 Volumes and flow rates of the chromatographic separation with the DGA resin using the prepFAST MC™ system

Step	Acid	Load and dispense volume (mL)	Load and dispense rate (mL min^{-1})
Conditioning	2 mol per L HNO_3	5	2
Load	2 mol per L HNO_3	1	1
Mg, Na, K	2 mol per L HNO_3	3	2
Sr	6 mol per L HNO_3	10	2
Ca	0.05 mol per L HCl	8	2
Wash	0.05 mol per L HCl	10 × 2	10 × 2

Table 3 Summary of volumes and acids used for the manually conducted chromatographic separation with AG50W-X12

Resin	Volume (mL)	Acid	Molarity (mol L^{-1})	Comment
AG50W-X12 (mesh 200–400)	5	HNO_3	1	Conditioning
	0.2	HNO_3	1	Sample load
	23	HNO_3	1	Wash
	8	HNO_3	1	K fraction
	1	HNO_3	1	"Pre-Mg"
	9	HNO_3	2	Mg fraction
	1	HNO_3	2	"Post-Mg"
	5	MQ-H_2O		Wash
	12	HCl	6	Wash

Table 4 Settings of the MC-ICP-MS and Apex 2G in the analytical session

Inlet system		APEX 2G	
Cool gas [L min^{-1}]	16	Ar sweep [mL min^{-1}]	323
Auxiliary gas [L min^{-1}]	0.8	Spraychamber [°C]	140
Sample gas [L min^{-1}]	0.9	Peltier cooler [°C]	3
Z [mm]	1.55		

onto 3 mL of resin (column length: 8 cm; diameter: 0.7 cm). Mg is eluted with the loading volume and 3 mL HNO_3 (2 mol L^{-1}). This fraction also contains K and Na, as well as Al, Mn, Rb and Ba. Sr is eluted with 10 mL HNO_3 (6 mol L^{-1}), followed by Ca that is eluted with 8 mL HCl (0.05 mol L^{-1}) (Fig. 1A). Table 2 lists the acid volumes and flow rates used. The chromatographic separation produces the following blanks in the respective fraction in which they were collected: Mg: (0.2 ± 0.07) ng, K: (4 ± 0.7) ng, Sr: (0.06 ± 0.03) ng and Ca: (40 ± 23) ng. Because Mg does not bind to the resin, it simply washes through, leading to a yield of 100%. Even though when the Mg amounts are minimized to a few micrograms to keep the total cations loaded low, the high Ca/Mg ratio of carbonates still causes a breakthrough of Ca. Approx. 40% of the cation exchange capacity of the DGA resin (0.45 meq) is used when 3–26 μg Mg of an aragonite sample are processed. The repetition of this first step overall removes 99.96% of the Ca which results in an overall decrease of Ca/Mg by roughly a factor of 1000. Fig. 1B shows the elution profile of the second separation. Between the two separations the samples are dried down and redissolved in 1 mL HNO_3 (2 mol L^{-1}). After the second separation, the samples are dried and redissolved in 200 μL HNO_3 (1 mol L^{-1}). The third chromatographic separation step serves to separate the remaining cations, in aragonite predominantly Na and K that have relatively high abundances (K/Mg: 40–90 mmol mol^{-1}; Na/Mg: 4.4–19 mol mol^{-1}). This is achieved by a manual separation in a clean lab using columns filled with 1.2 mL of AG50W-X12 (200–400 mesh) resin (column length: 6.1 cm; diameter: 0.5 cm). The precleaned sample of 0.23–27 mg carbonate uses approx. 0.5% of the cation exchange capacity (2.5 meq). The samples are loaded onto the column and flushed with 23 mL HNO_3 (1 mol L^{-1}) to release Na. The following 8 mL of HNO_3 (1 mol L^{-1}) contain the K fraction (Fig. 2). The next millilitre is collected separately to monitor possible tailing of K and Mg ("pre-Mg" fraction). Mg is then collected in the following 9 mL HNO_3 (2 mol L^{-1}). One millilitre is added and collected separately to monitor possible Mg tailing at the end of the Mg elution peak ("post-Mg" fraction).

The column is then cleaned with 12 mL HCl (6 mol L^{-1}). Fig. 2 shows an elution profile of a solution containing each 2 μg

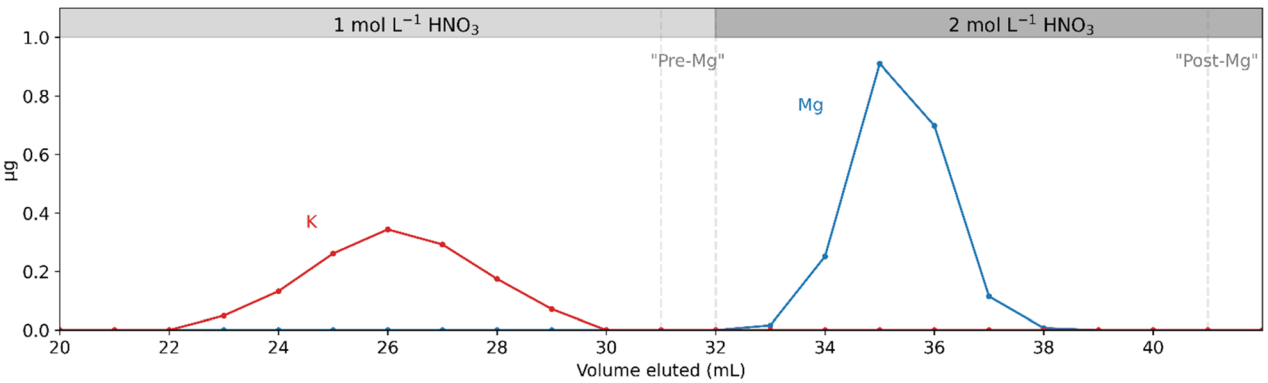

Fig. 2 Elution profile of the chromatographic separation of a K–Mg solution (1 : 1) with the AG50W-X12 (200–400 mesh) resin. Bao *et al.*, 2020 have shown, that Na elutes within the first 20 mL.

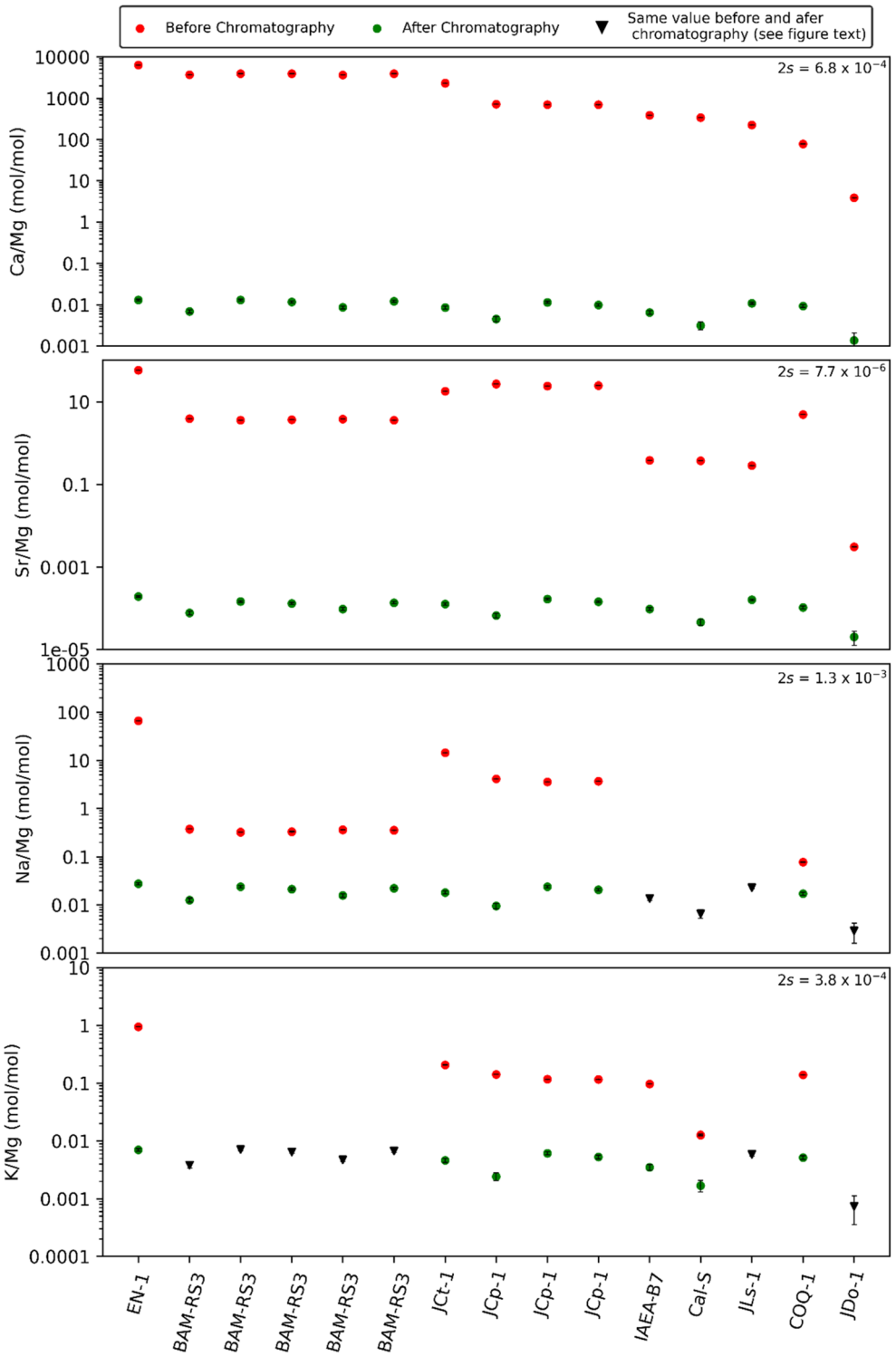

Fig. 3 Mg/element ratios of the standards before and after all three chromatographic separations. Concentration measurements were conducted using ICP-OES. After chromatography all elements other than Mg occur at concentrations below LOD. Therefore, the Mg/element ratios are calculated using the LOD. In some standards the Na and K concentrations are <LOD before chromatography; these are shown as black triangles.

Mg and K separated using AG50W-X12. This third separation also removes any remaining Ca, further purifying the sample. In this separation we achieve Mg yields of (99.6 ± 0.2)% to (100 ± 0.2)%. The uncertainty is assumed based on the yields of the repeated measurements of JCp-1. The pre- and post-Mg fractions contain <2.5 ng Mg. The K fraction has an average blank of about (44 ± 12) ng K and blanks in the Mg fraction average (6 ± 7) ng Mg. Following chromatographic separations, samples are dried down and redissolved in 3 mL HNO_3 (0.32 mol L^{-1}), of which a 1 mL aliquot is used to determine the Mg concentration by ICP-OES. The complete rundown of the three chromatographic separations is shown in Tables 2 and 3.

Mg isotope measurement

Mg isotope ratios were determined in low resolution mode on a Thermo Scientific Neptune Plus™ multicollector inductively coupled plasma mass spectrometer (MC-ICP-MS) in the Geochemistry Department at the University of Göttingen. Samples and the bracketing standard DSM-3 were diluted to 0.25 μg per mL Mg in HNO_3 (0.32 mol L^{-1}). Concentrations were matched to within 10%. Sample solutions were nebulised with a microconcentric PFA nebuliser with an effective uptake rate of 70 μL min^{-1} and the aerosol was dried using an APEX-2G (Elemental Scientific Inc.). Measurements were done using a Ni sample cone and H type skimmer cone. Intensities of ^{24}Mg, ^{25}Mg and ^{26}Mg were measured in Faraday cups connected to 10^{11} Ω resistors (other settings listed in Table 4). Under these conditions a sensitivity of 16 V ^{24}Mg per 1 μg per mL Mg was achieved. To correct for instrumental mass fractionation and drift, we applied the sample-standard-bracketing method using DSM-3 as bracketing standard. Blank measurements were performed before and after every two samples. The blank contributed <0.28% of the signal intensity. Instrumental drift in the measurement session (13 hours) amounted only to 0.36‰ and 0.64‰ for $\delta^{25}Mg$ and $\delta^{26}Mg$. The introduction of non-purified samples could impact the accuracy of $\delta^{26}Mg$ values. A significant amount of matrix elements would lead to a mismatching matrix with the bracketing standard, resulting in variable mass bias, the introduction of Ca leads to an isobaric interference of doubly charged $^{48}Ca^{2+}$ on ^{24}Mg. However, due to the low abundance of the ^{48}Ca isotope (0.187%) and low formation rates of doubly charged Ca ions (0.1%),[32] even a relatively high concentration of residual Ca in the purified solutions, *e.g.* 25 μg mL^{-1} (corresponding to a Ca/Mg ratio of 0.1) would result in a bias of only 0.002‰ and can therefore be neglected.

Results

The presented purification process for Ca-rich samples yields pure solutions. Following chromatography, all elements except Mg yielded non-detectable concentrations. To determine Mg/element ratios for those samples, the limit of detection (LOD: blank + three times the standard deviation) was considered as the maximum concentration. The detection limits for the analysis were 15 ng per mL Ca, 1 ng per mL Mg, 0.1 ng per mL Sr, 53 ng per mL Na and 9.7 ng per mL K. We show the resulting Mg-to-element ratios that decreased significantly during the chromatographic separation (Fig. 3). Ca/Mg and Sr/Ca decreased by roughly five orders of magnitude. Na/Mg and K/Mg ratios were lowered by approx. 1–3 orders of magnitude. The isotope ratios of the analysed standards (Table 5) yield identical δ-values compared to published values (Fig. 4).

Mg isotope ratios for the standards IAEA-B7 and BAM-RS3 are reported here for the first time. We report the 2*s* analytical repeatability of measurements from one analytical session for 1 to 4 digestions of sample material ranging from 0.23 to 26.91 mg, containing 3.12 to 25.99 μg Mg (see Table 5). IAEA-B7 was measured at $\delta^{25}Mg_{DSM3} = (-2.34 \pm 0.02)$‰ and $\delta^{26}Mg_{DSM3} = (-4.50 \pm 0.06)$‰ (1 digestion of 3.57 mg). BAM-RS3 was measured at an average $\delta^{25}Mg_{DSM3} = (-1.58 \pm 0.02)$‰ (SE) and a $\delta^{26}Mg_{DSM3}$ of (−3.02 ± 0.04)‰ (SE) ($N = 4$).

Table 5 Results of the Mg isotope ratio measurements. The standards BAM-RS3 and JCp-1 were digested and separated four and three times, respectively. *N* is the number of repeat measurements in the same analytical session

Standard	$\delta^{25}Mg$ (‰ DSM3)	2*s*	$\delta^{26}Mg$ (‰ DSM3)	2*s*	*N*	Mass (mg)	Mg (μg)	Mg recovery (%)	$\delta^{25}Mg_{Lit.}$[a] (‰ DSM3)	2*s*	$\delta^{26}Mg_{Lit.}$[a] (‰ DSM3)	2*s*
BAM-RS3	−1.51	0.05	−2.88	0.06	4	17.38	3.13	99.6 ± 0.2				
	−1.60	0.01	−3.04	0.04	4	19.73	3.55	99.6 ± 0.2				
	−1.59	0.02	−3.05	0.07	4	26.91	4.84	99.7 ± 0.2				
	−1.62	0.02	−3.12	0.06	4	18.68	3.36	99.6 ± 0.2				
JCt-1	−1.74	0.03	−3.40	0.03	4	14.17	4.52	99.7 ± 0.2	−1.72	0.01	−3.37	0.01
EN-1	−2.25	0.05	−4.38	0.08	4	26.50	2.79	99.5 ± 0.2	−2.23	0.02	−4.39	0.02
IAEA-B7	−2.34	0.02	−4.50	0.06	4	3.57	6.58	99.8 ± 0.2				
JCp-1	−1.05	0.05	−2.03	0.08	4	8.30	8.00	99.8 ± 0.2	−1.03	0.02	−1.96	0.04
	−1.04	0.03	−2.02	0.04	4	3.23	3.12	99.6 ± 0.2	−1.03	0.02	−1.96	0.04
	−1.04	0.02	−2.01	0.02	4	3.87	3.73	99.6 ± 0.2	−1.03	0.02	−1.96	0.04
Cal-S	−2.29	0.02	−4.37	0.10	4	5.80	12.80	99.9 ± 0.2	−2.25	0.11	−4.37	0.14
JLs-1	−1.97	0.06	−3.79	0.13	4	1.13	4.14	99.6 ± 0.2	−1.86	0.05	−3.60	0.07
COQ-1	−0.29	0.05	−0.55	0.07	4	1.97	14.23	99.7 ± 0.2	−0.25	0.04	−0.50	0.06
JDo-1	−1.21	0.01	−2.34	0.05	4	0.23	25.99	100 ± 0.2	−1.23	0.09	−2.35	0.15

[a] For references to the literature values see Table 1.

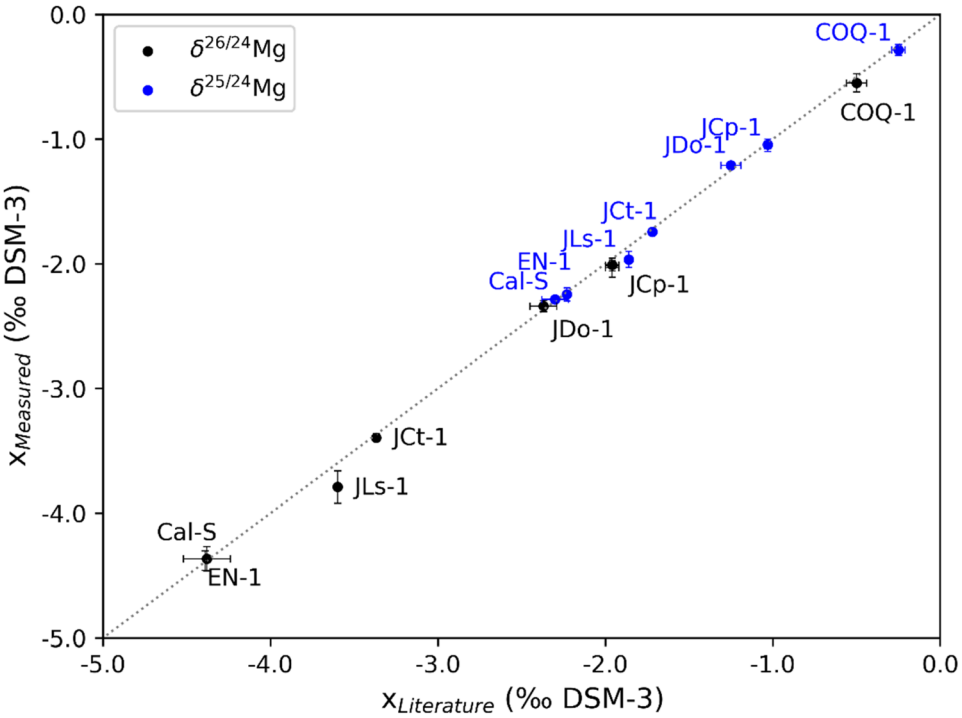

Fig. 4 δ^{26}Mg and δ^{25}Mg values of the measured standards plotted against published values. Error bars show the 2*s* analytical repeatability.

Discussion

The presented method for chromatographic Mg separation from calcium carbonates allows quantitative Mg recovery and a high degree of purification. The Mg isotope ratios of the standards agree with the published values within the analytical reproducibility (Fig. 4A), except for the JLs-1, which we measured with a deviation of (0.19 ± 0.06)‰ δ^{26}Mg. An explanation for this deviation might be that either the reference value or our value is biased due to Mg-loss or an elevated column blank. The AG50W-X12 resin used for the separation is prone to the loss of isotopically light Mg, when the Mg-peak is cut-off too early, causing a shift towards higher δ^{26}Mg values, because of isotopic fractionation on AG50W-X12 (ref. 3 and 32) releases ^{26}Mg first. The standard BAM-RS3 was measured with four replicates. One out of the four analyses show a deviation that exceeds the analytical reproducibility of typically (−1.61 ± 0.03)‰ δ^{25}Mg and (−3.07 ± 0.07)‰ δ^{26}Mg. One possible explanation is that this standard is not homogenous in Mg isotopes on this sample size (17.38 to 26.91 mg). Alternatively, an undetected contamination of Mg could have biased the analysis. This highlights that the work with low Mg amounts is sensitive to procedural blanks and hence requires careful handling. The cumulative procedural blanks sum up to (6.2 ± 7.07) ng. We note that high purity of the separation improves the analytical results by allowing very steady instrumental mass fractionation.

Conclusion

The use of the automated prepFAST MC™ system minimises labour substantially and provides an efficient way to remove the bulk Ca from calcium carbonate samples. Additionally, the automated system allows for a reduction of operator-induced errors and allows collecting the Sr fraction from the same aliquot. Mg, Ca and Sr blanks are very low despite repeated usage of the same resin batch (200 times). The reproducibility of Mg isotope ratios in separate digestions, each containing <8 μg Mg demonstrates the reliable and precise determination of Mg isotope ratios in calcium carbonate.

Data availability

The data supporting this article have been included in the main article.

Conflicts of interest

The authors declare no conflict of interest.

Notes and references

1 A. Galy, M. Bar-Matthews, L. Halicz and R. K. O'Nions, *Earth Planet. Sci. Lett.*, 2002, **201**, 105–115.
2 A. Immenhauser, D. Buhl, D. Richter, A. Niedermayr, D. Riechelmann, M. Dietzel and U. Schulte, *Geochim. Cosmochim. Acta*, 2010, **74**, 4346–4364.
3 V. T. C. Chang, A. Makishima, N. S. Belshaw and R. K. O'Nions, *J. Anal. At. Spectrom.*, 2003, **18**, 296–301.
4 A. Brenot, C. Cloquet, N. Vigier, J. Carignan and C. France-Lanord, *Geochim. Cosmochim. Acta*, 2008, **72**, 5070–5089.
5 F. Wombacher, A. Eisenhauer, A. Heuser and S. Weyer, *J. Anal. At. Spectrom.*, 2009, **24**, 627.

6 M. S. Fantle and J. A. Higgins, *Geochim. Cosmochim. Acta*, 2014, **142**, 458–481.
7 A. Geske, R. H. Goldstein, V. Mavromatis, D. K. Richter, D. Buhl, T. Kluge, C. M. John and A. Immenhauser, *Geochim. Cosmochim. Acta*, 2015, **149**, 131–151.
8 M. S. Fantle, B. D. Barnes and K. V. Lau, *Annu. Rev. Earth Planet. Sci.*, 2020, **48**, 549–583.
9 Z. Hu, Z. Shi, G. Li, Z. Xia, L. Yi, C. Liu and W. Li, *Earth Planet. Sci. Lett.*, 2022, **595**, 117755.
10 D. Bi, S. Zhai, D. Zhang, X. Liu, A. Dong and X. Shi, *J. Asian Earth Sci.*, 2024, **261**, 105981.
11 A. S. C. Ahm, C. J. Bjerrum, C. L. Blättler, P. K. Swart and J. A. Higgins, *Geochim. Cosmochim. Acta*, 2018, **236**, 140–159.
12 F. Teng, *Rev. Mineral. Geochem.*, 2017, **82**, 219–287.
13 A. Sadekov, N. S. Lloyd, S. Misra, J. P. D'Olivo and M. McCulloch, *Rapid Commun. Mass Spectrom.*, 2020, **34**(23), e8918.
14 C. Saenger and Z. Wang, *Quat. Sci. Rev.*, 2014, **90**, 1–21.
15 P. A. E. Pogge von Strandmann, J. Forshaw and D. N. Schmidt, *Biogeosciences*, 2014, **11**, 5155–5168.
16 D. Hippler, D. Buhl, R. Witbaard, D. K. Richter and A. Immenhauser, *Geochim. Cosmochim. Acta*, 2009, **73**, 6134–6146.
17 F. Wombacher, A. Eisenhauer, F. Böhm, N. Gussone, M. Regenberg, W. C. Dullo and A. Rüggeberg, *Geochim. Cosmochim. Acta*, 2011, **75**, 5797–5818.
18 T. Yoshimura, M. Tanimizu, M. Inoue, A. Suzuki, N. Iwasaki and H. Kawahata, *Anal. Bioanal. Chem.*, 2011, **401**, 2755–2769.
19 F. Planchon, C. Poulain, D. Langlet, Y. M. Paulet and L. André, *Geochim. Cosmochim. Acta*, 2013, **121**, 374–397.
20 J. A. Higgins and D. P. Schrag, *Earth Planet. Sci. Lett.*, 2015, **416**, 73–81.
21 A. M. Gothmann, J. Stolarski, J. F. Adkins and J. A. Higgins, *Geology*, 2017, **45**, 1039–1042.
22 R. A. Berner, A. C. Lasaga and R. M. Garrels, *Am. J. Sci.*, 1983, **283**, 641–683.
23 M. E. Tucker and S. J. Jones, *Sedimentary Petrology*, John Wiley & Sons, 2023.
24 E. T. Tipper, A. Galy, J. Gaillardet, M. J. Bickle, H. Elderfield and E. A. Carder, *Earth Planet. Sci. Lett.*, 2006, **250**, 241–253.
25 C. Zong, Z. Bao, X. Nie, Y. Zhang, K. Chen and H. Yuan, *J. Anal. At. Spectrom.*, 2021, **36**, 273–278.
26 L. Ma, Y. Sun, Z. Jin, Z. Bao, P. Zhang, Z. Meng, H. Yuan, X. Long, M. He and K.-J. Huang, *Geochim. Cosmochim. Acta*, 2019, **259**, 1–16.
27 T. Gao, S. Ke, R. Li, X. Meng, Y. He, C. Liu, Y. Wang, Z. Li and J. Zhu, *Rapid Commun. Mass Spectrom.*, 2019, **33**, 767–777.
28 Z. Wang, P. Hu, G. Gaetani, C. Liu, C. Saenger, A. Cohen and S. Hart, *Geochim. Cosmochim. Acta*, 2013, **102**, 113–123.
29 E. B. Bolou-Bi, N. Vigier, A. Brenot and A. Poszwa, *Geostand. Geoanal. Res.*, 2009, **33**, 95–109.
30 Z. Bao, C. Zong, K. Chen, N. Lv and H. Yuan, *Int. J. Mass Spectrom.*, 2020, **448**, 116268.
31 A. Pourmand and N. Dauphas, *Talanta*, 2010, **81**(3), 741–753.
32 M. Tatzel, J. Vogl, M. Rosner, M. J. Henehan and T. Tütken, *Anal. Chem.*, 2019, **91**, 14314–14322.
33 S. Tonarini, M. Pennisi, A. Adorni-Braccesi, A. Dini, G. Ferrara, R. Gonfiantini, M. Wiedenbeck and M. Gröning, *Geostand. Newsl.*, 2003, **27**, 21–39.
34 J. S. Ray, K. Pande, R. Bhutani, A. D. Shukla, V. K. Rai, A. Kumar, N. Awasthi, R. S. Smitha and D. K. Panda, *Contrib. Mineral. Petrol.*, 2013, **166**, 1613–1632.
35 GeoReM Database, **http://georem.mpch-mainz.gwdg.de/**.